Supplementary Information for "Mechanisms driving Subpolar North Atlantic Upper Ocean Heat Content Predictability in CMIP6 Decadal Prediction Systems"

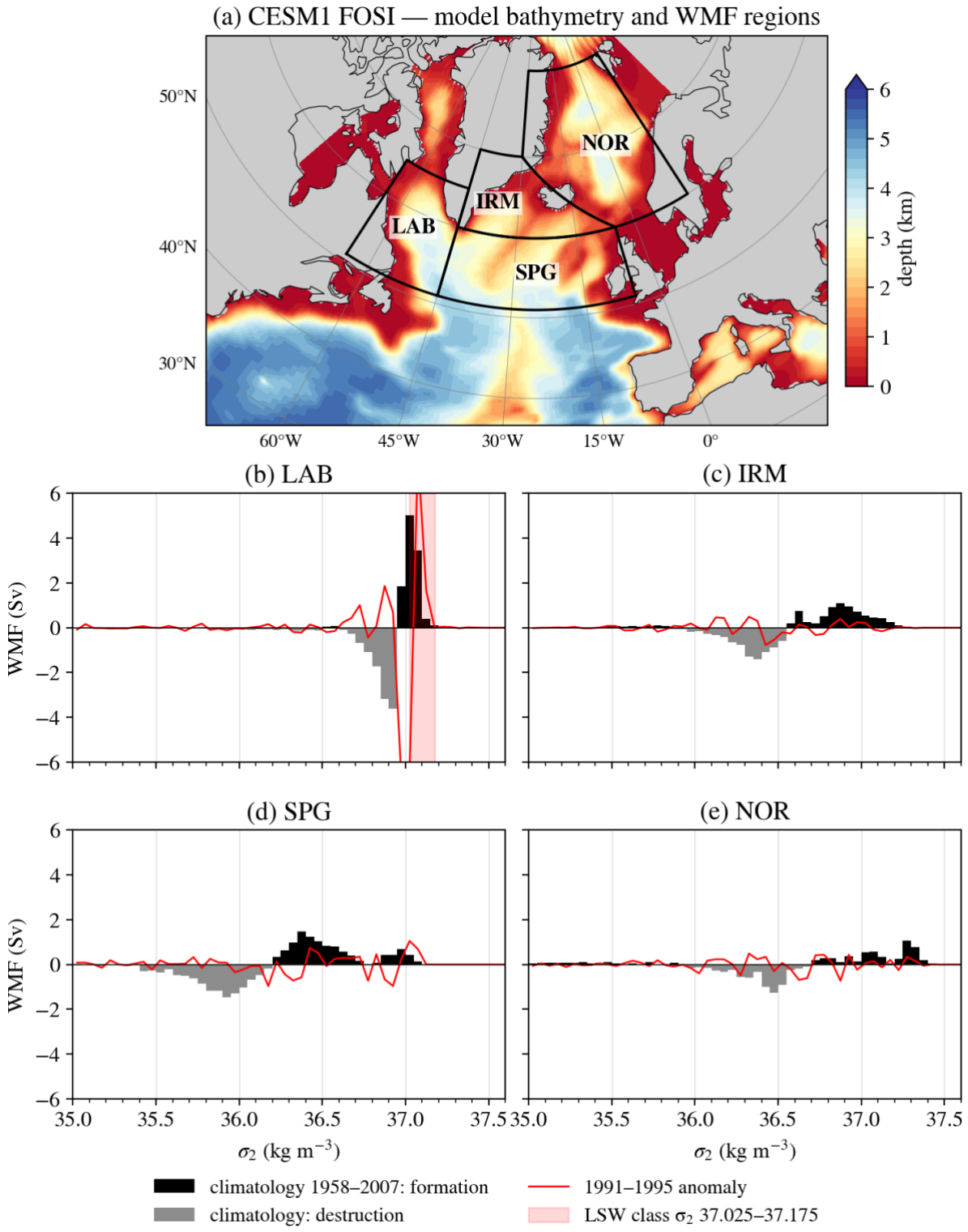


Figure S1: Surface water mass transformation (WMF) from CESM1 FOSI. a) Model bathymetry with regions used in WMF calculation highlighted. b-e) 1958-2007 mean surface WMF as a function of density class, with thin red lines indicating the 1991-1995 anomaly.

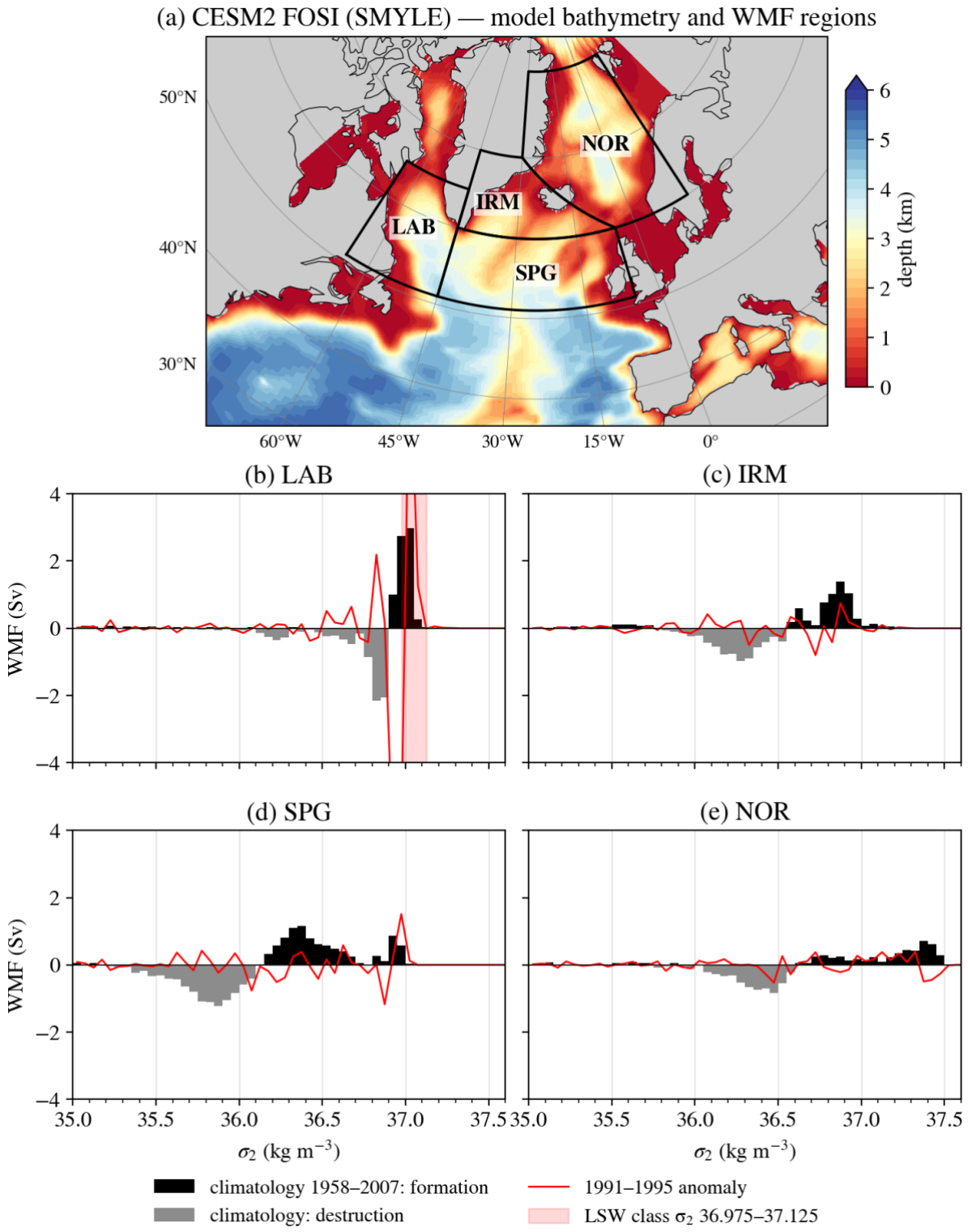


Figure S2: Same as Fig. S1 but for CESM2 FOSI (SMYLE).

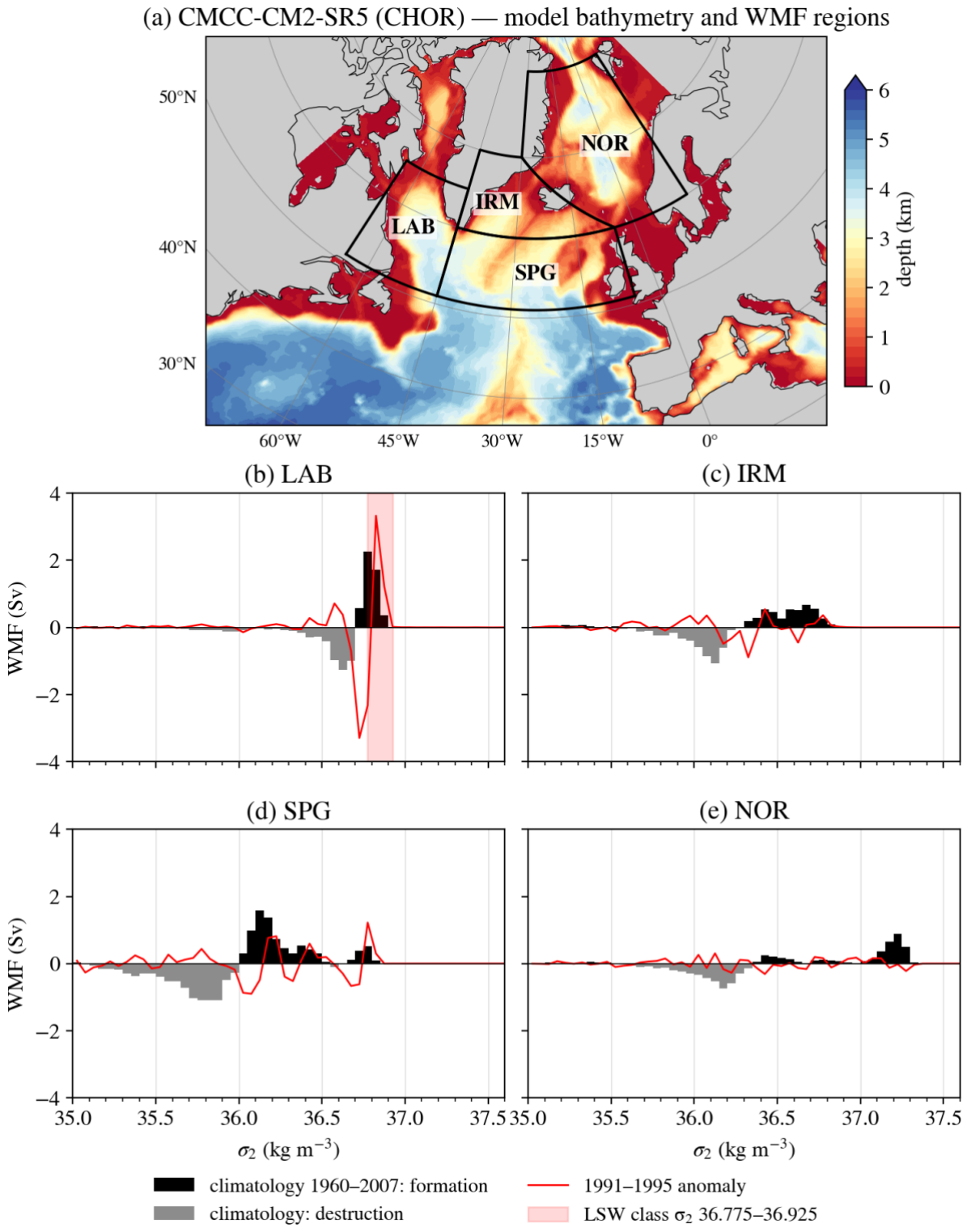


Figure S3: Same as Fig. S1 but for CMCC-CM2-SR5's initialisation dataset.

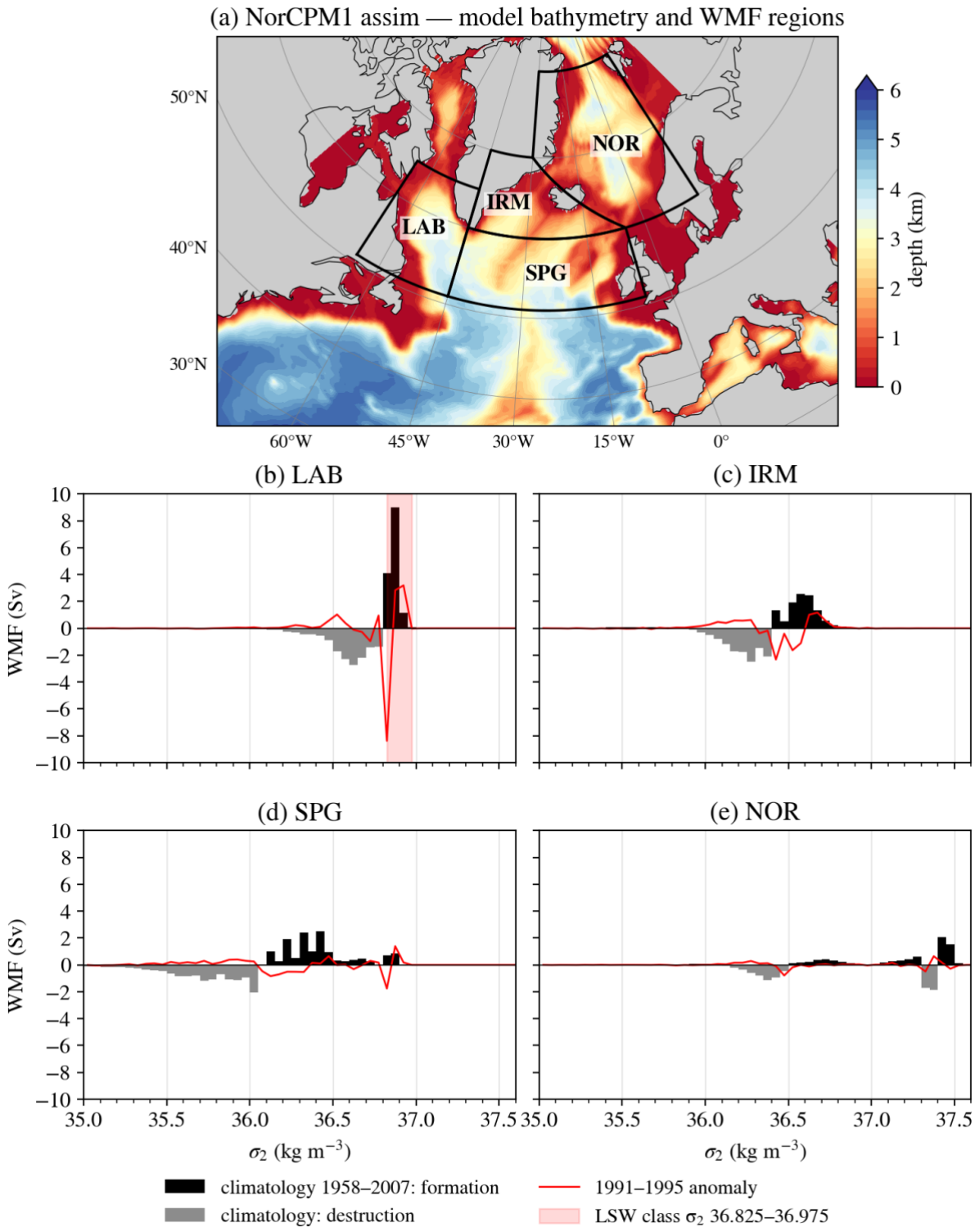


Figure S4: Same as Fig. S1 but for NorCPM1 assim.

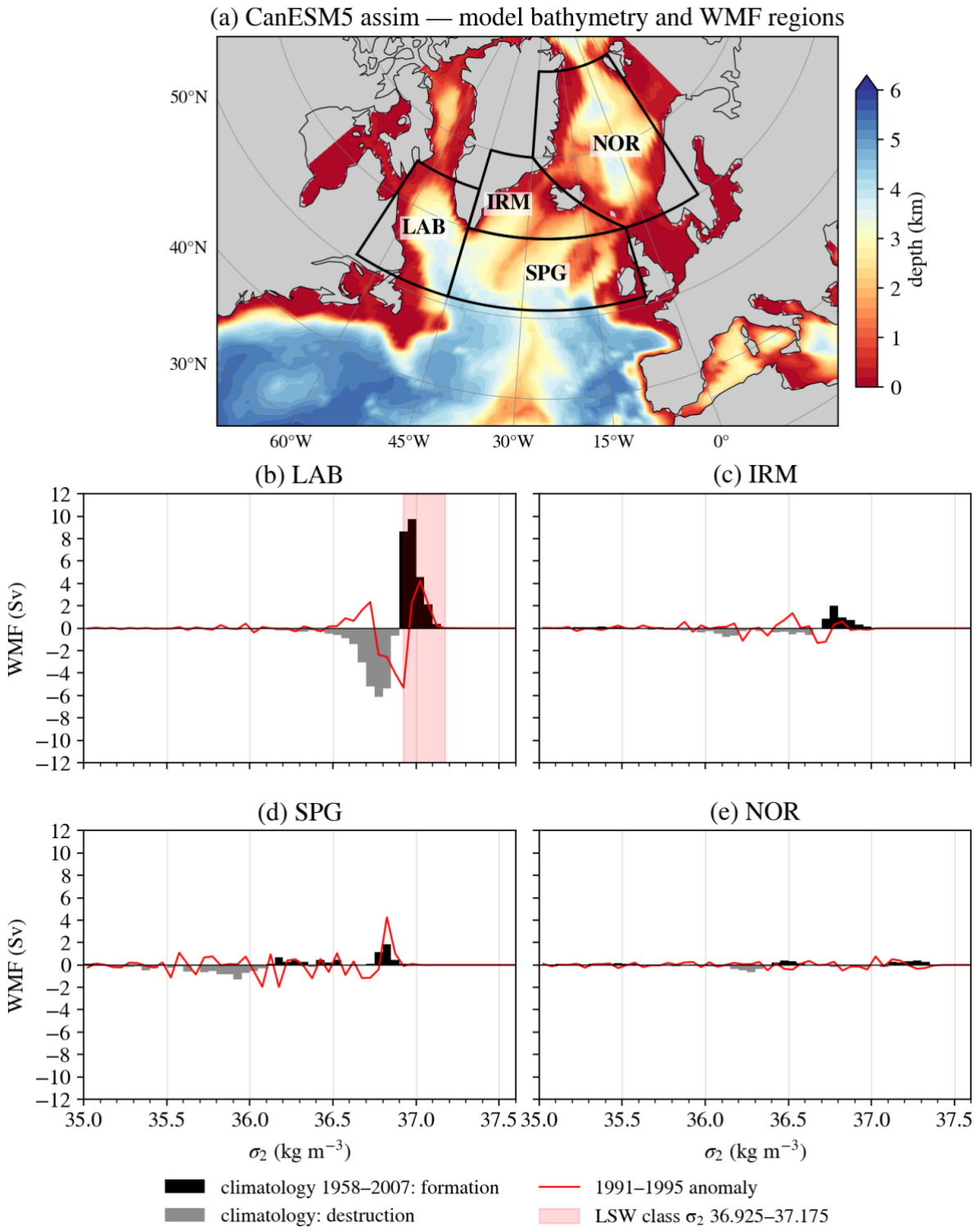


Figure S5: Same as Fig. S1 but for CanESM5 assim.

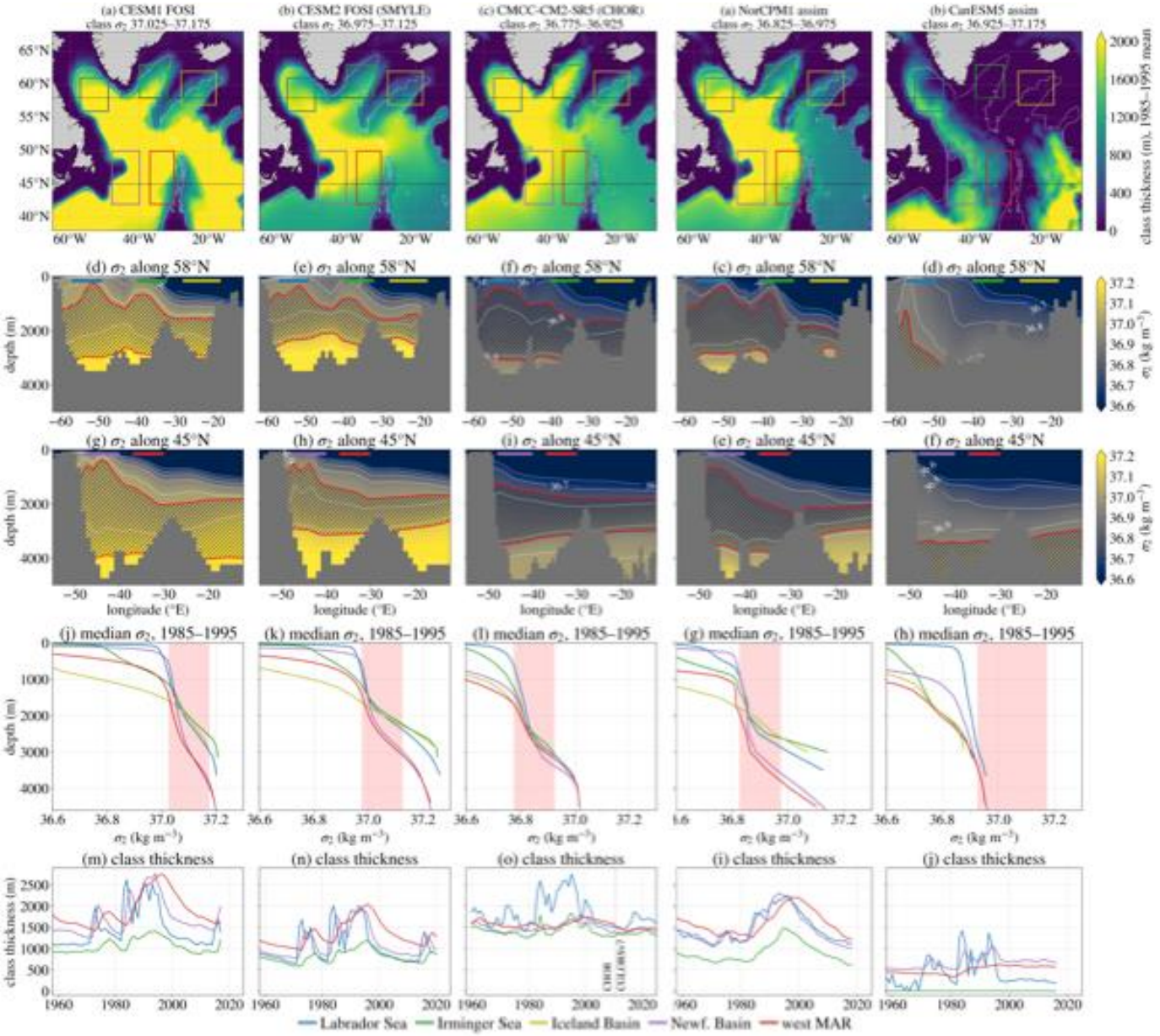


Figure S6: Where each model's LSW density class sits, and how it spreads from the Labrador Sea, in the initialization dataset for each decadal prediction system for CESMI FOSI (column 1), CESM2 FOSI (SMYLE, column 2), CMCC-CM2-SR5 (column 3), NorCPM1 (column 4) and CanESM5 (column 5). Each model's σ_2 class is taken from the positive limb of surface water-mass formation in its initialization run, and is given in the column titles. First row: 1985-1995 mean thickness of the class (m), from interpolated isopycnal depths. Coloured boxes mark the analysis regions: Labrador Sea (56-61°N, 57-49°W), Irminger Sea (58-63°N, 40-32°W), Iceland Basin (57-62°N, 28-18°W), Newfoundland Basin (42-50°N, 48-40°W), and the western half of the Mid-Atlantic Ridge (MAR) box of Yeager, 2020 (42-50°N, 37-30°W). Coloured dashed lines mark the sections in the second and third rows. The white dashed contours represent the 2500 m isobath (ETOP02), which outlines the MAR. Second and third rows: 1985-1995 mean σ_2 (kg m-3) along 58°N (Labrador Sea - Irminger Sea - Iceland Basin) and along 45°N (Newfoundland Basin - MAR). The density class of the LSW layer is hatched, with its bounding isopycnals in red. White contours are every 0.1 kg m-3. Coloured bars along the top show where each section crosses the regions. Grey is the

model's own bathymetry. Fourth row: median 1985-1995 σ_2 profiles in each region, using water columns deeper than 1500 m. Pink shading shows the class. Fifth row: annual-mean class thickness (m) averaged over the Labrador Sea, Irminger Sea, Newfoundland Basin and western MAR, 1958-2025. In CMCC-CM2-SR5 the dotted line marks the switch from CHOR to CGLORSV7 at 2010.

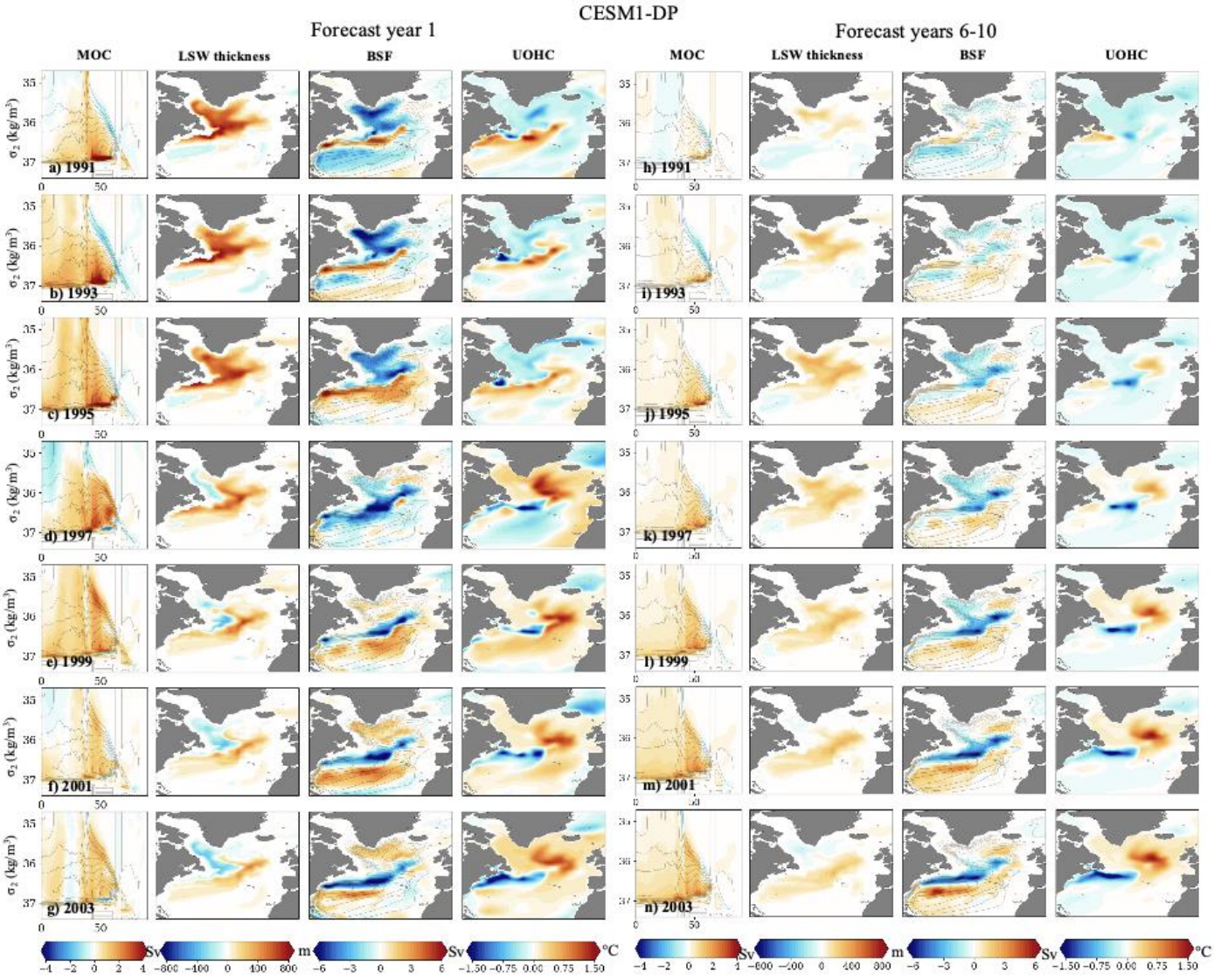


Figure S7: Contour plots for CESM1-DP showing the time evolution of MOC, LSW thickness, BSF and UOHC at forecast year 1 (left panels) and forecast years 6-10 (right panels).

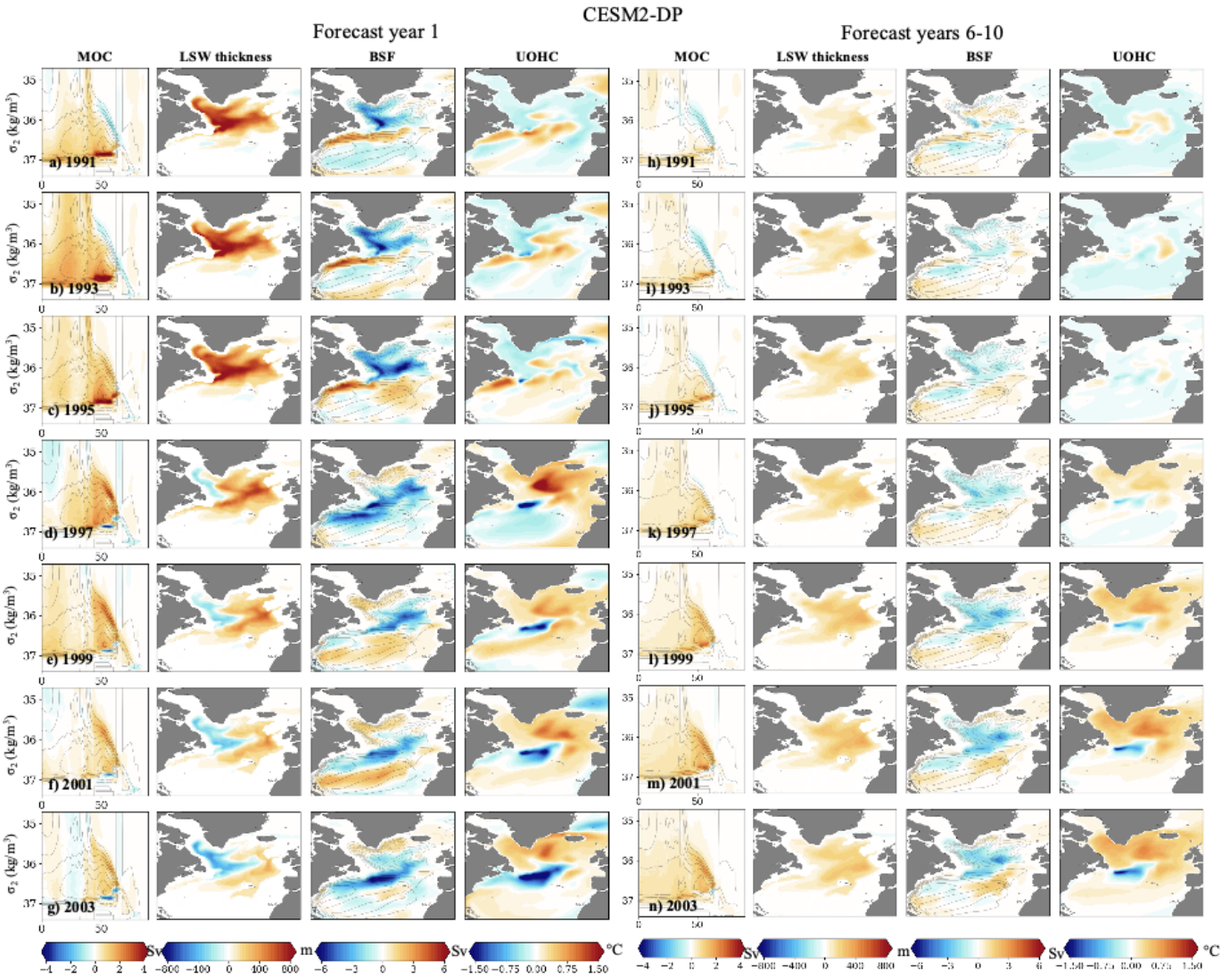


Figure S8: Contour plots for CESM2-DP showing the time evolution of MOC, LSW thickness, BSF and UOHC at forecast year 1 (left panels) and forecast years 6-10 (right panels).

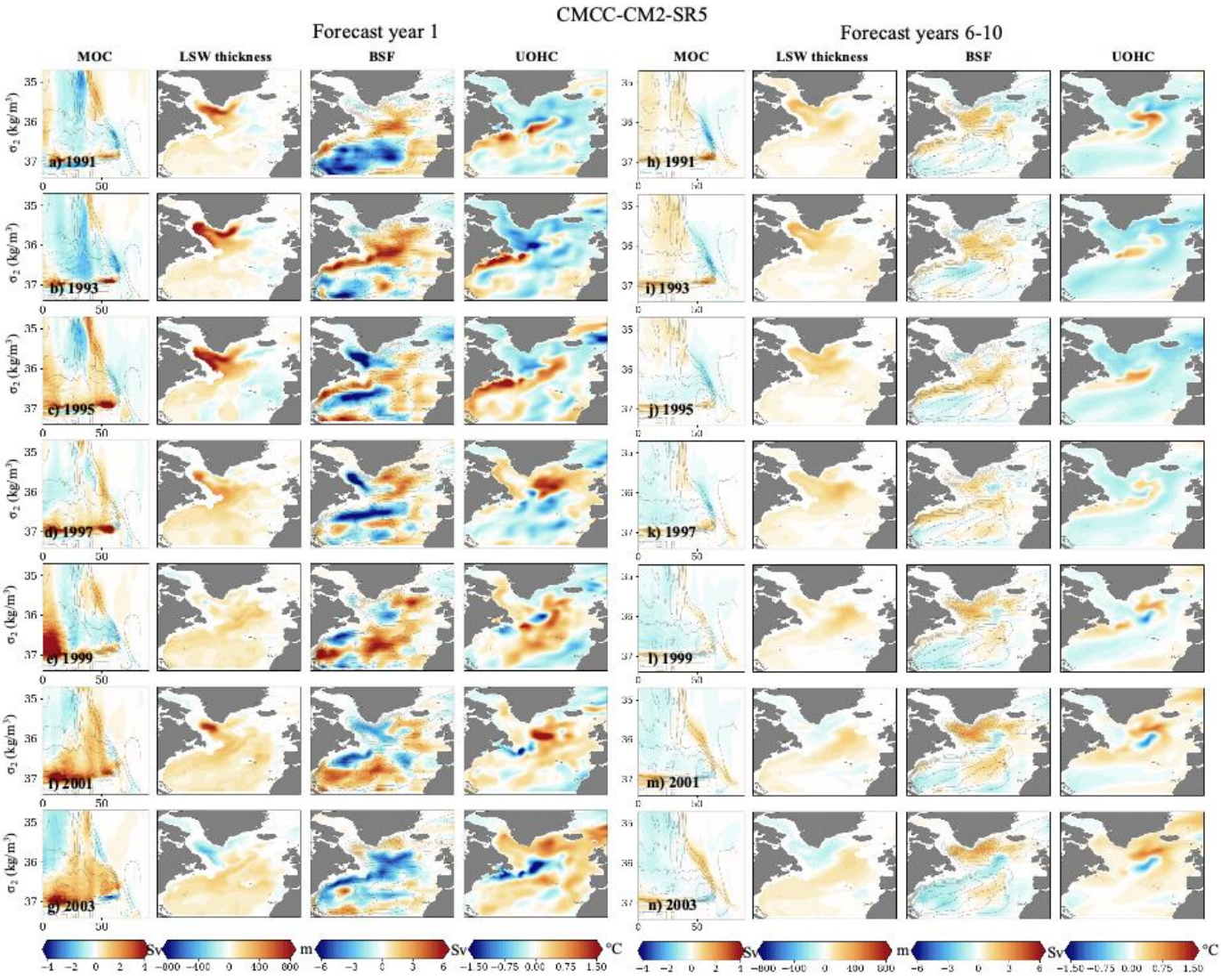


Figure S9: Contour plots for CMCC-CM2-SR5 showing the time evolution of MOC, LSW thickness, BSF and UOHC at forecast year 1 (left panels) and forecast years 6-10 (right panels).

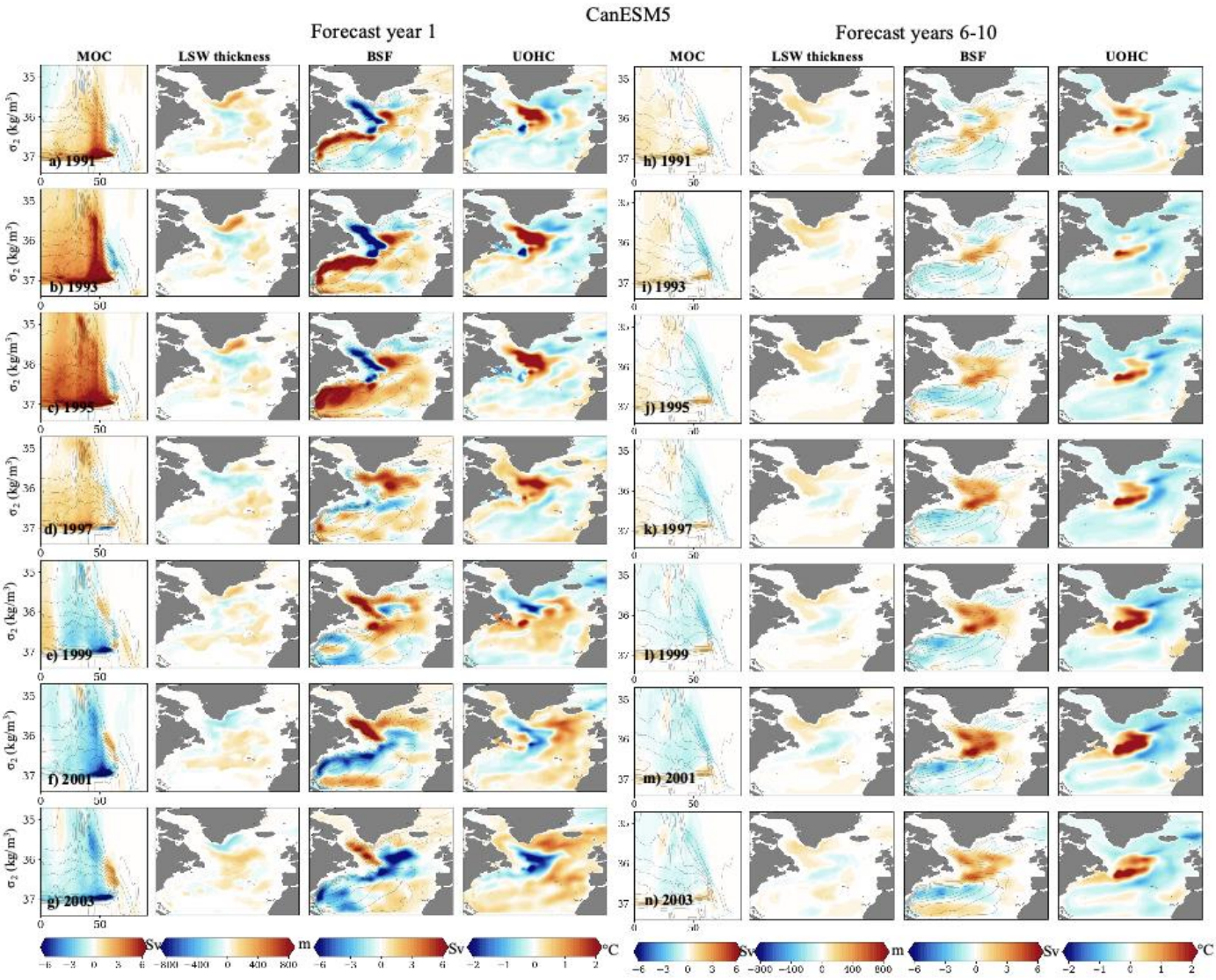


Figure S10: Contour plots for CanESM5 showing the time evolution of MOC, LSW thickness, BSF and UOHC at forecast year 1 (left panels) and forecast years 6-10 (right panels).

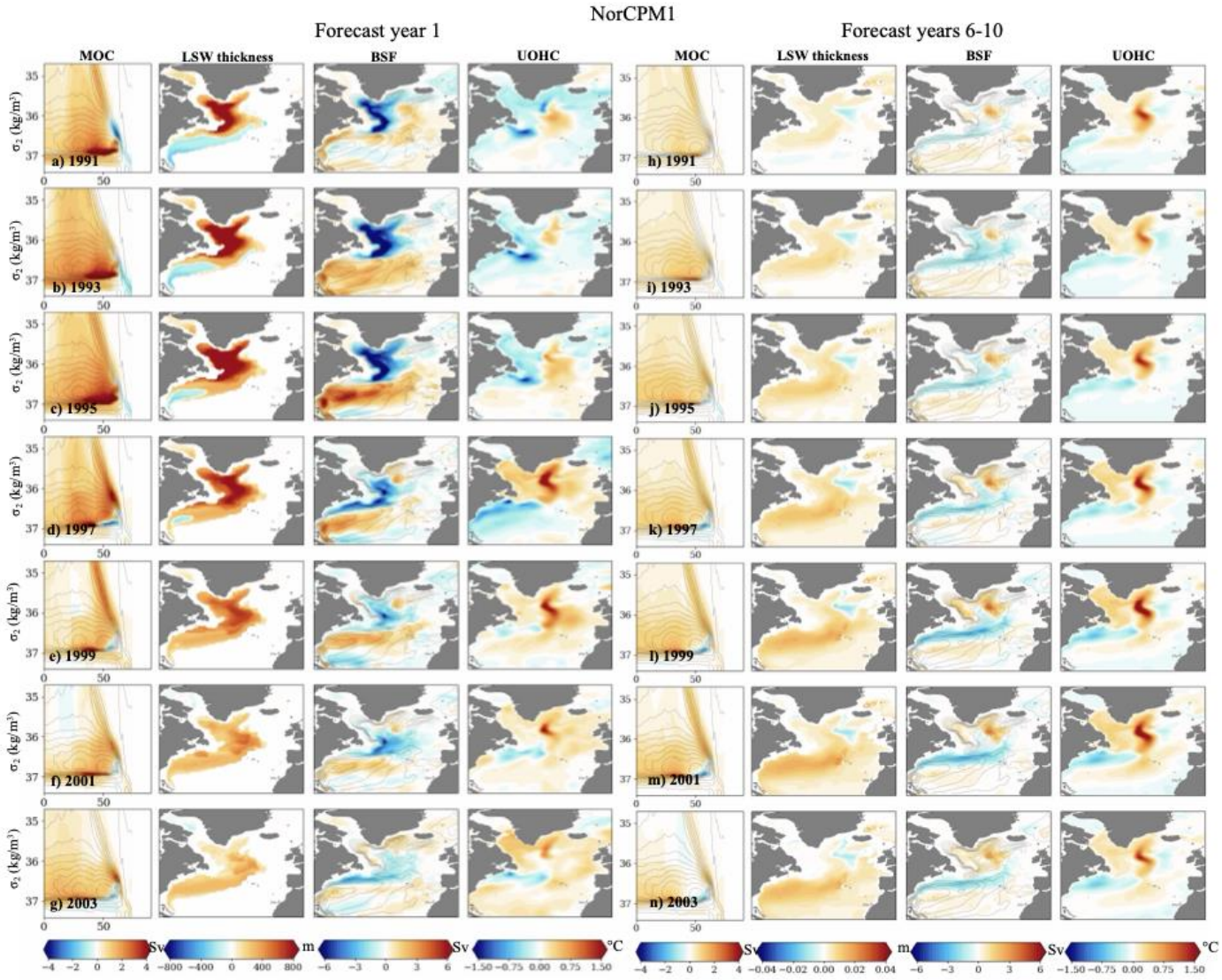


Figure S11: Contour plots for NorCPM1 showing the time evolution of MOC, LSW thickness, BSF and UOHC at forecast year 1 (left panels) and forecast years 6-10 (right panels).

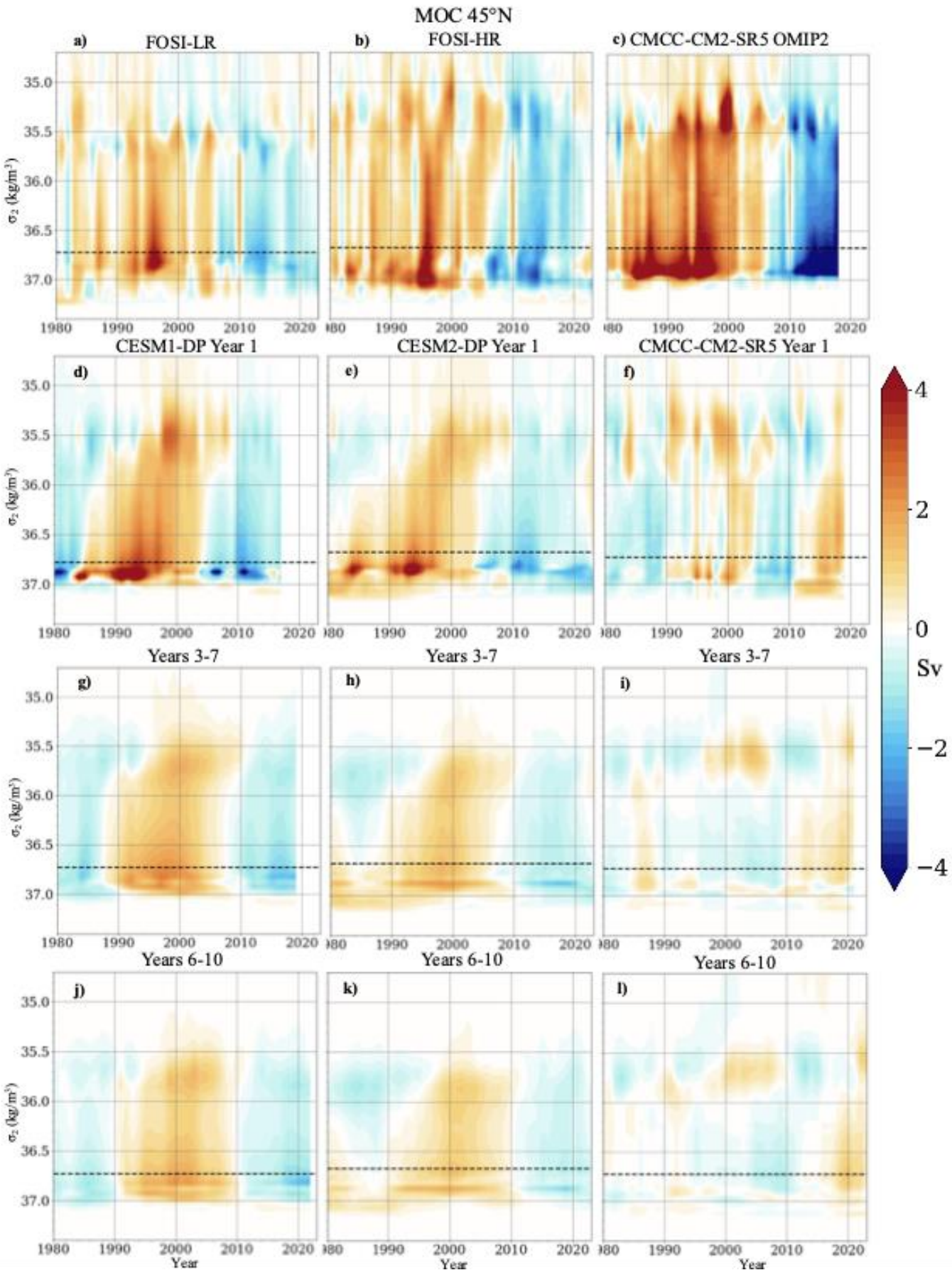

MOC 45°N
a) FOSI-LR
b) FOSI-HR
c) CMCC-CM2-SR5 OMIP2
CESM1-DP Year 1
CESM2-DP Year 1
CMCC-CM2-SR5 Year 1
Years 3-7
Years 6-10
d)
e)
f)
g)
h)
i)
j)
k)
l)
σ2 (kg/m3)
35.0
35.5
36.0
36.5
37.0
1980
1990
2000
2010
2020
Year
4
2
0
−2
−4
Sv

Figure S12: Same as Figure 5 but with FOSI-LR-B and FOSI-HR-B swapped for FOSI-LR and FOSI-HR, which include interannual wind variability.

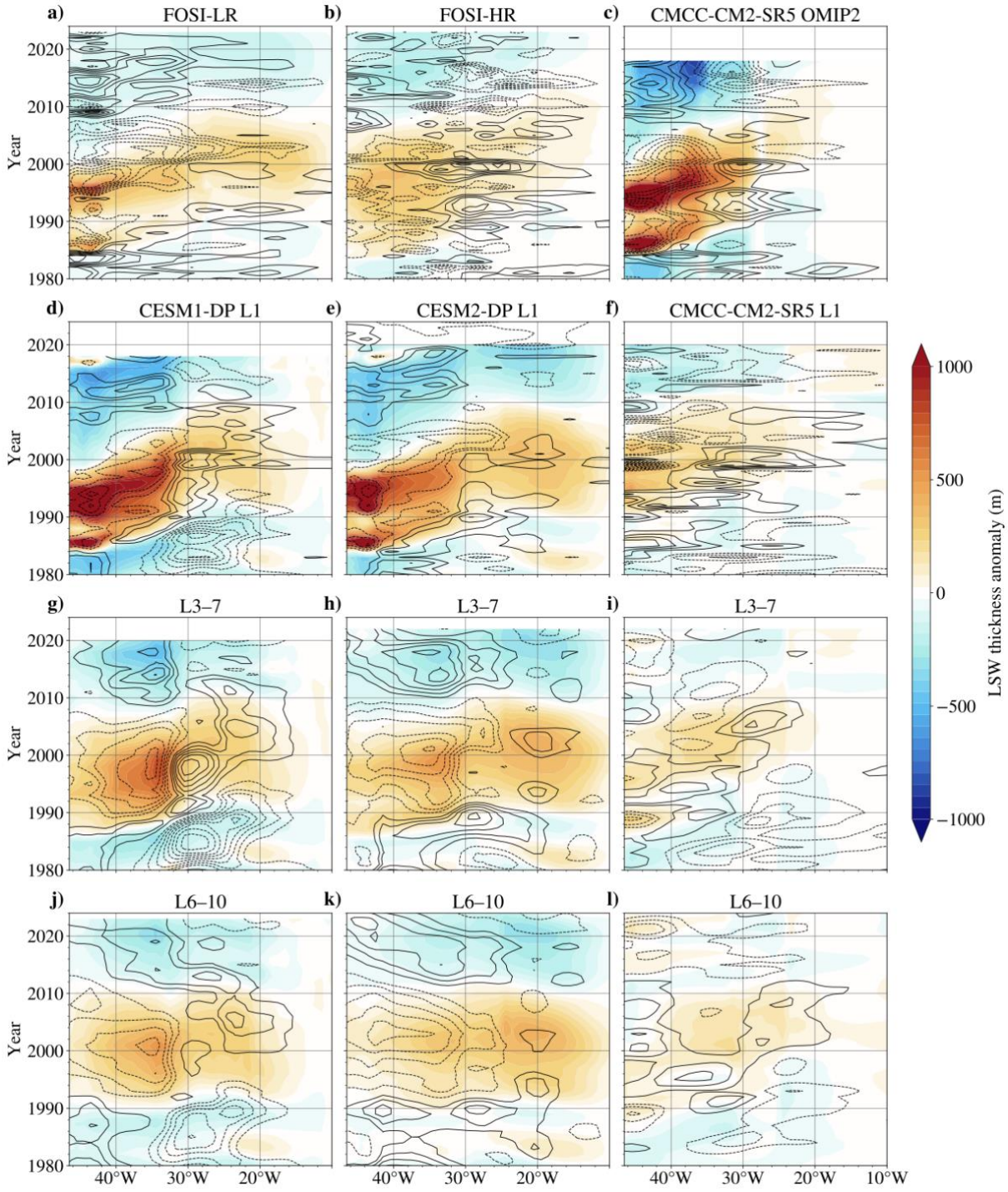


Figure S13: Same as Figure 6 but with FOSI-LR-B and FOSI-HR-B swapped for FOSI-LR and FOSI-HR, which include interannual wind variability.

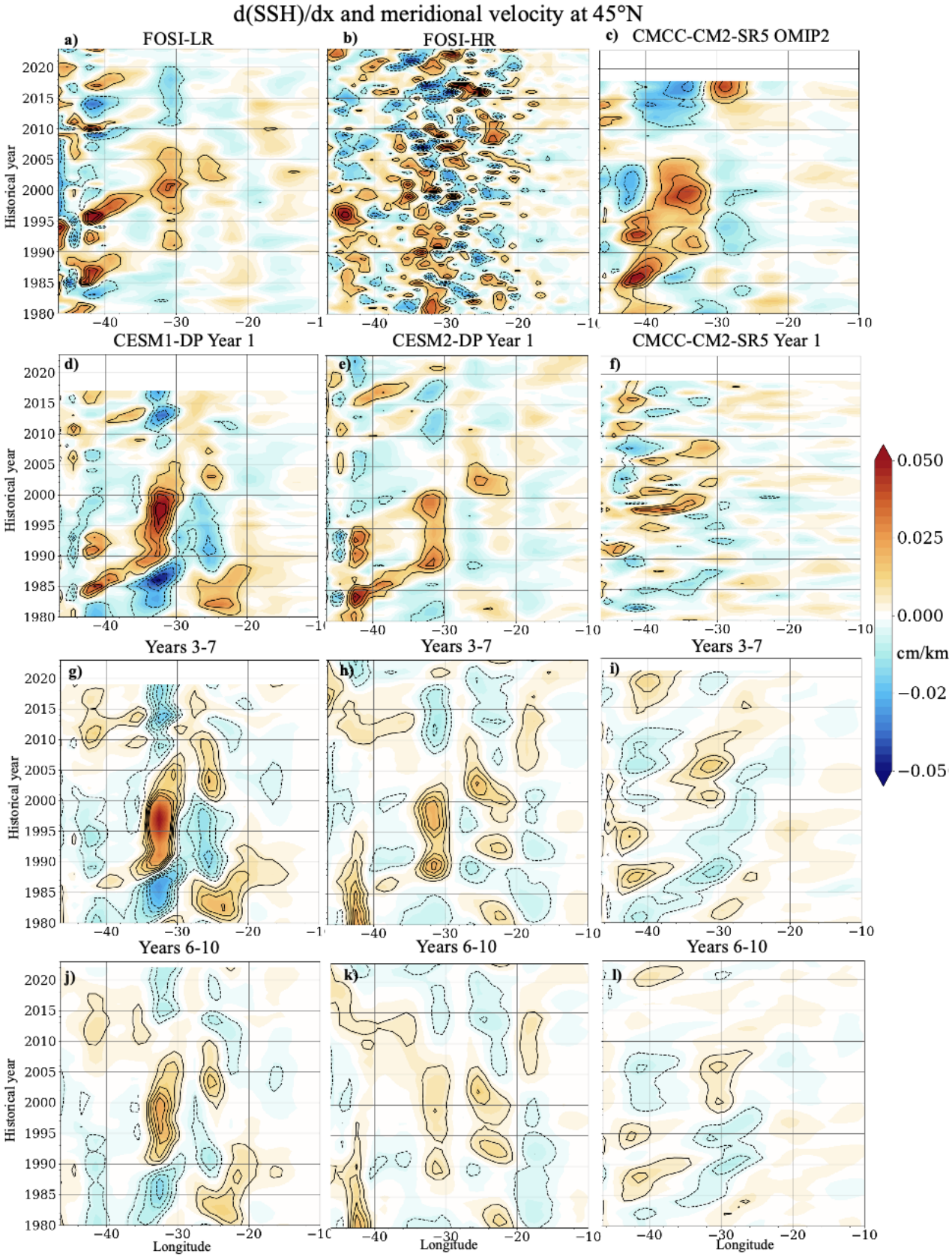


Figure S14: Same as Figure 7 but with FOSI-LR-B and FOSI-HR-B swapped for FOSI-LR and FOSI-HR, which include interannual wind variability.

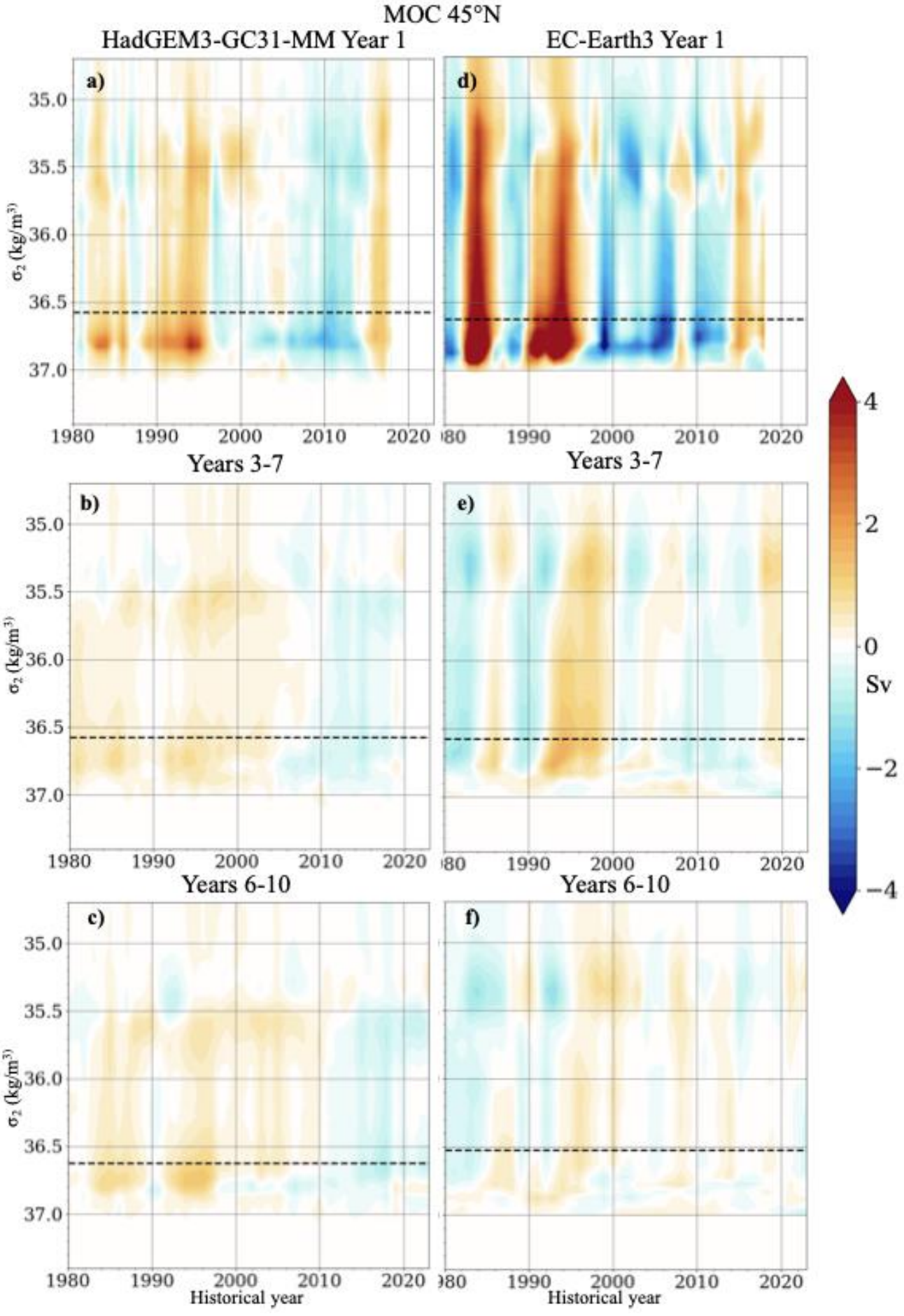

MOC 45°N
HadGEM3-GC31-MM Year 1
EC-Earth3 Year 1
a)
d)
b)
e)
c)
f)
Years 3-7
Years 3-7
Years 6-10
Years 6-10
σ2 (kg/m3)
35.0
35.5
36.0
36.5
37.0
1980
1990
2000
2010
2020
Historical year
4
2
0
Sv
−2
−4

Fig. S15: Same as Fig. 5 but for medium skill models.

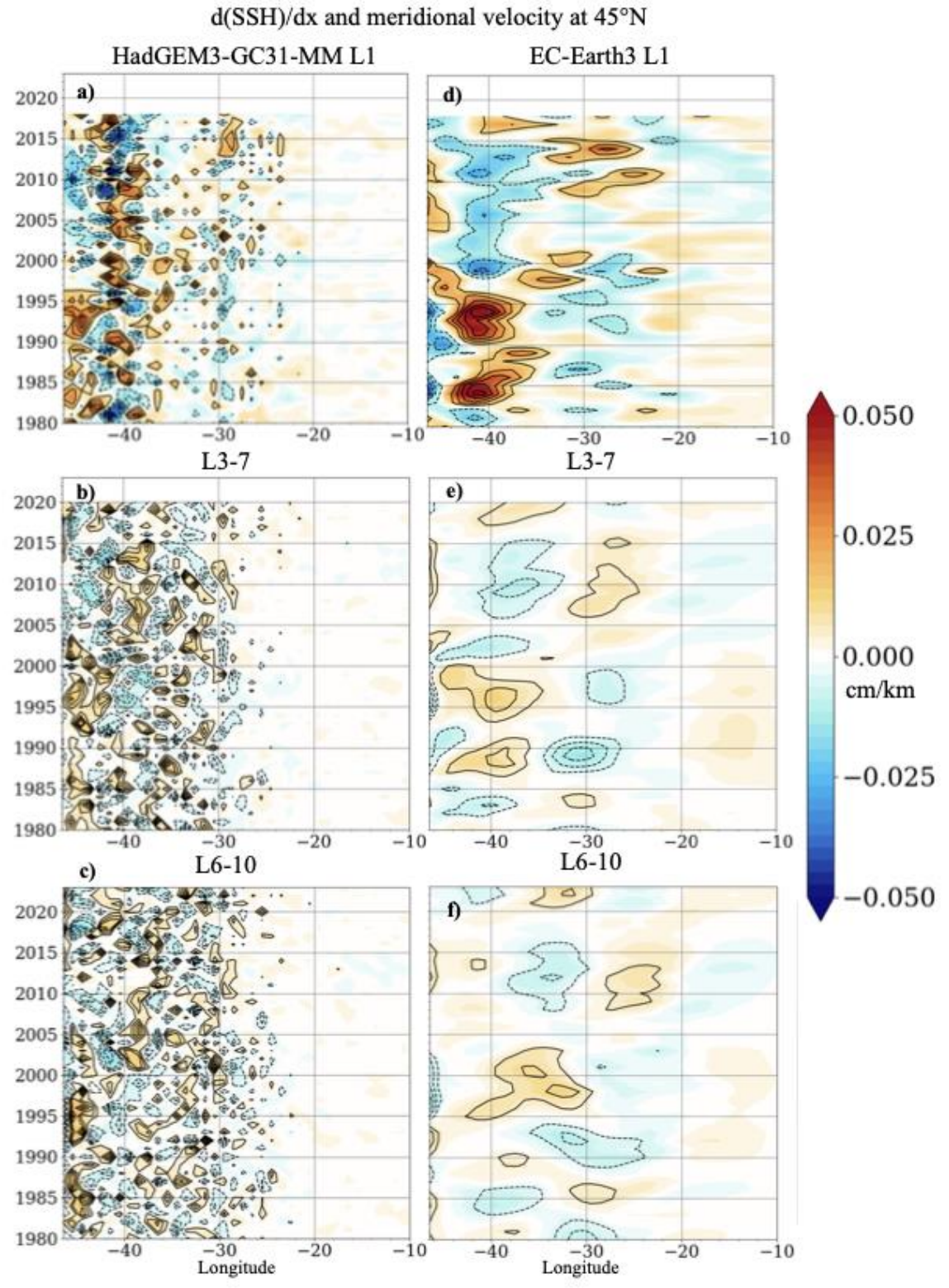


Fig. S16: Same as Fig. 7 but for medium skill models.